

Biogenic controls on the air–water carbon dioxide exchange in the Sundarban mangrove environment, northeast coast of Bay of Bengal, India

H. Biswas, S. K. Mukhopadhyay, and T. K. De

Department of Marine Science, Calcutta University, 35 B.C. Road, Calcutta 700019, India

S. Sen

Department of Chemistry, Calcutta University, 92 A.P.C. Road, Calcutta 700009, India

*T. K. Jana*¹

Department of Marine Science, Calcutta University, 35 B.C. Road, Calcutta 700019, India

Abstract

The Sundarban mangrove forest (4,264 km²) constitutes about 3% of the total area of the world mangrove. We measured diurnal and seasonal variations of air–water CO₂ exchange in relation to the occurrence of phytoplankton during January–December 2001. Diurnal variations of airflows showed that the minimum and maximum CO₂ flux of $-16.2 \mu\text{mol m}^{-2} \text{h}^{-1}$ and $49.9 \mu\text{mol m}^{-2} \text{h}^{-1}$, respectively, occurred during the higher sea breeze. The average ratio of dissolved inorganic nitrogen (DIN = $13.85 \pm 7.19 \mu\text{mol L}^{-1}$) to dissolved inorganic phosphorus (DIP = $1.23 \pm 0.57 \mu\text{mol L}^{-1}$) was 11 ± 4 and the surface water was undersaturated with respect to dissolved oxygen. The mean value of 0.1 ± 0.08 for the ratio of phytoplankton production (P) to community respiration (R) indicated that the ecosystem was heterotrophic. The saturation of dissolved carbon dioxide with respect to the atmosphere varied seasonally between 59% and 156%, with minimum levels in postmonsoon and maximum levels in premonsoon/early monsoon (June/July). Out of the 36 genera of diatoms, 1 blue green alga, and 3 dinoflagellates that occurred throughout the year, only 6 reached bloom proportions in postmonsoon, when mangrove water was a sink of atmospheric CO₂. Although 59.3% of the emitted CO₂ was removed from the atmosphere by biological processes, on an annual basis, the Sundarban mangrove forest supplies $13.8 \text{ kg C ha}^{-1} \text{ yr}^{-1}$ of CO₂ from water surface to the atmosphere. Even though it is important to compare all in and out fluxes, there is no direct link between CO₂ emission and the later CO₂ removal by biological processes.

The difference between the sources ($7.0 \pm 1.2 \times 10^{12} \text{ kg yr}^{-1}$, fossil fuel combustion and deforestation) and sinks ($5.4 \pm 0.8 \times 10^{12} \text{ kg yr}^{-1}$, atmosphere and ocean) of $1.6 \times 10^{12} \text{ kg yr}^{-1}$ for atmospheric CO₂ is very close to the overall uncertainty ($\pm 1.4 \times 10^{12} \text{ kg yr}^{-1}$) of estimation (Millero 2000). The missing carbon sink could be the result of uncertainty in flux estimates. The estimated ocean sink values obtained from the ocean model (Quay et al. 1992) and atmospheric model (Tans et al. 1990) showed considerable deviation. Little direct proof is available to support this estimate. Schimel et al. (1995) observed wide variation of net oceanic uptake of CO₂ in the range between 17% and 39% of the fossil fuel emission. Normal source and sink strength of a forest with respect to CO₂ could be changed due to deforestation and fertilization by CO₂. Land use change would also affect the carbon stocks in woods and soils. Anthropogenic processes, responsible for the conversion of a productive estuary to a heterotrophic one (Frankignoulle et al. 1998; Mukhopadhyay et al. 2002a), further complicate the uncertainty of the estimation of unaccounted sinks.

Sometimes it is not clear if an ecosystem is a net source or sink of CO₂ (Mukhopadhyay et al. 2002b). The sink characteristics of an ecosystem depend on solubility and biological pump for CO₂. The solubility pump depends on wind velocity, temperature, salinity, and dissociation of carbonic acid. The biological pump is primed in surface waters by the production of plant material. However, the production of calcifying and noncalcifying phytoplankton has a different impact on CO₂ air–water exchange. While the latter drive the organic carbon pump, which causes the draw down of CO₂ in the surface ocean, the former contributes to the calcium carbonate pump, which in contrast, releases CO₂ in the environment (Riebesell et al. 2000). Coastal ocean accounts for about 14% of global ocean production (IGBP 1995) and anthropogenically driven changes are of more interest in coastal areas. The anthropogenic flux of dissolved nutrients from land to coastal ocean is now equal to and in some areas greatly in excess of the natural flux. Mangrove forest belongs to the major ecosystem of the biosphere and about 60–75% of tropical coasts are fringed by this highly productive ecosystem (Clough 1998). Nutrient outwelling from mangroves can exceed riverine fluxes and may have a considerable influence on the productivity in coastal waters (Dittmar and Lara 2001). This may result in blooming of phytoplankton and may change the efficiency of the biological pump. Again, river runoff can also cause the considerable dilution of coastal water, which can change the solubility pump. Therefore, coastal oceans could have highly variable source–

¹ Corresponding author (tkjana@hotmail.com).

Acknowledgments

Authors (H.B. and S.K.M.) are grateful to the Department of Ocean development and Council of Scientific and Industrial Research, India, for providing fellowship. Helpful suggestions by two anonymous reviewers are gratefully acknowledged.

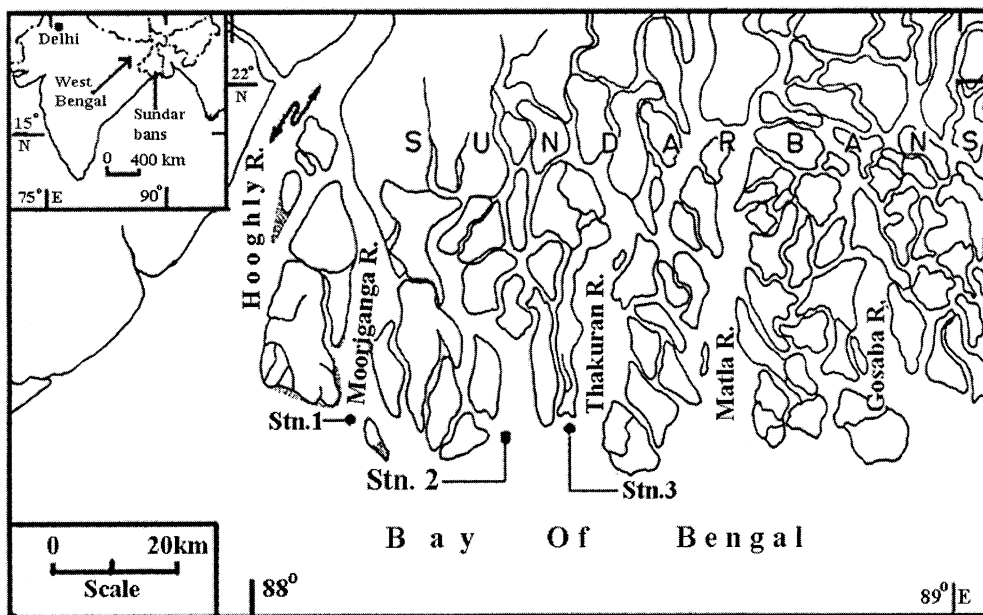


Fig. 1. Station locations in the Sundarban mangrove ecosystem.

sink strength for CO_2 and play an important role in determining whether the whole ocean is autotrophic or heterotrophic (Kempe and Pelger 1991). Hope et al. (2001) cautioned that direct measurements of land-atmosphere CO_2 gas exchange that ignored waterborne fluxes might significantly overestimate terrestrial accumulation. There are few systematic studies on the chemistry and flux of CO_2 in the mangrove waters (Ghosh et al. 1987). Most biogeochemical studies in the mangrove waters have found nutrient and organic carbon fluxes (Ayukai et al. 1998; Dittmar and Lara 2001). Despite mangroves being the most abundant ecosystem of the tropical coasts, relatively little is known about their role in the carbon cycle. Sundarban mangrove ecosystem, North East coast of the Bay of Bengal, India, has been the focus of ecological and biogeochemical studies for several decades (Misra et al. 1985; Ghosh et al. 1990; Roy et al. 2000). The present study was intended to identify diurnal and seasonal variations and the driving forces behind the CO_2 exchange from the Sundarban mangrove water.

Sites and methods

Study site—The Indian Sundarban ($21^\circ32'$ and $22^\circ40'N$; $88^\circ05'$ and 89^\circE) is the estuarine phase of the River Ganges (Fig. 1) and comprises $9,630 \text{ km}^2$, out of which $4,264 \text{ km}^2$ of intertidal area, covered with thick mangroves, is subdivided as forest subecosystem and $1,781 \text{ km}^2$ of water area as aquatic subecosystem. The rest has been reclaimed for human settlement and agricultural purposes. It is a unique bioclimatic zone in land-ocean boundaries of the northeastern coast of the Bay of Bengal and the largest delta on the globe. East to west, this area is about 140 km in length and extends approximately $52\text{--}70 \text{ km}$ from the sea level to the far north. This estuarine phase has been under increasing stress due to the construction of barrage at Farakka (300 km from the sea end of the Hooghly River), port activities at

Haldia and Calcutta, dredging, and discharge of sewage from Haldia and Calcutta metropolis.

Sampling and measurements—For flux measurements at three stations in the northeast coast of the Bay of Bengal off Mooriganga, Saptamukhi, and Thakuran estuaries, three distributaries of the River Ganges, surface water samples were collected from the middle of the mouth of each estuary at 3-h intervals for 24 h at each site. Sampling was continued for 3 consecutive d from full moon in every 4 weeks between January and December 2001 (Fig. 1), covering three seasons: monsoon (June–September), postmonsoon (October–January), and premonsoon (February–May). Air samples were collected from 10 m above the water surface with the help of a portable air sampler (APS 2 Lawrence and Mayo) at a rate of 2 L min^{-1} and drawn into gas sampling bulbs in triplicate, which were evacuated before collection. The air temperature, atmospheric moisture content, atmospheric pressure, and wind velocity were also recorded by using temperature, moisture probes and an anemometer connected with a computerized weather station (Model No. DAVIS 7440).

Micrometeorological sensors were mounted 10 m above the water surface using a bamboo pole from an anchored mechanized boat. The fugacity of CO_2 in air [$f_{\text{CO}_2(\text{air})}$] was measured with a gas chromatograph (Shimadzu 14B). A methanizer MTN-1 was used for catalytic reduction of CO_2 to CH_4 at 350°C over shimalite Ni catalyst followed by its subsequent determination with flame ion detector (FID). Calibration gas, supplied by Eurassian Associates, had mole fraction of 318 ppm in nitrogen. The relative uncertainty (standard deviation relative to mean value) on f_{CO_2} measurements was found to be ± 0.063 . The measured concentration of CO_2 was converted to fugacity using the virial equation of state (Weiss 1974).

Water samples for CO_2 fugacity [$f_{\text{CO}_2(\text{water})}$] were collected

in separate glass bottles and were preserved with HgCl₂ for analysis back in the laboratory. The $f_{\text{CO}_2(\text{water})}$ was determined by equilibrating the samples with nitrogen (Millero 2000). The CO₂ in the equilibrated nitrogen was measured using gas chromatography with relative uncertainty of ± 0.073 . The $f_{\text{CO}_2(\text{water})}$ was calculated from the mixing ratio of CO₂, atmospheric pressure and the Weiss formula (Weiss 1974). Alkalinity was determined by potentiometric titration with 0.1 N HCl in a closed cell at 25°C after Bradshaw and Brewer (1988) using micro pH meter (Systronics, Model No. 362).

A Gran plot was made of the data points after the second equivalence point. Calibration was performed against standard seawater ($\text{TCO}_2/\text{TA} = 0.93$). A standard deviation of 0.08% for total alkalinity was obtained. Dissociation constants of Goyet and Poisson (1989) were used to calculate the concentration of HCO₃⁻ normalized to salinity 35 ($\text{NHCO}_3^- = \text{HCO}_3^- \times 35/S$). Secchi disc was used to measure transparency of the water column. Salinity was determined by Mohr–Knudsen titration and standard seawater of chlorinity 19.374 procured from the National Institute of Oceanography, Goa, was used for standardization ($S = 1.80655 \times \text{Cl}$). Water samples from a Niskin bottle were allowed to flow through the glass bottle of 125-ml capacity until the bottle was finally filled and Winkler titration was performed for the determination of dissolved oxygen. Nutrients were analyzed by spectrophotometric methods. Standard procedures detailed in Grasshoff (1983) were followed and a relative error of accuracy was $\pm 2\%$ for dissolved inorganic phosphorus (DIP), $\pm 3\%$ for nitrate, $\pm 5.8\%$ for ammonia, and $\pm 6\%$ for silicate. The detection limits were 0.05 $\mu\text{mol L}^{-1}$ for DIP, 0.1 $\mu\text{mol L}^{-1}$ for dissolved inorganic nitrogen (DIN), and silicate. Gross primary production (P) and community respiration (R) were measured in situ by light- and dark-bottle method described by Strickland and Parson (1972).

Phytoplankton was collected from surface water using bolting silk 20- μm plankton net. For quantitative estimation, 1-liter water samples were preserved with Lugol's iodine solution and buffered formaldehyde.

After 24 h of sedimentation, the supernatant was rejected and the plankton counts, identifications, and cell radii were made from the settled material using a Sedgwick rafter counting chamber (Hasle and Syvertsen 1997). Shannon–Weaver index (H') (Shannon and Weaver 1963) was used to calculate the species diversity of phytoplankton. Cell volume was determined (Kellar et al. 1980) by using the simplest geometric configuration that best fit the shape of the cell being measured. Average measurements from 20 individuals of each species for each sampling period were considered. The total biovolume (V) of any species was calculated by multiplying the average cell volume in μm^3 by the number per liter. Total wet algal volume was computed as

$$V_t = \sum_{i=1}^n (N_i \times V_i)$$

where V_t is the total plankton cell volume in $\text{mm}^3 \text{L}^{-1}$, N_i is the number of organisms of the species L^{-1} , and V_i is the average volume of cells of the i th species in μm^3 . Flux den-

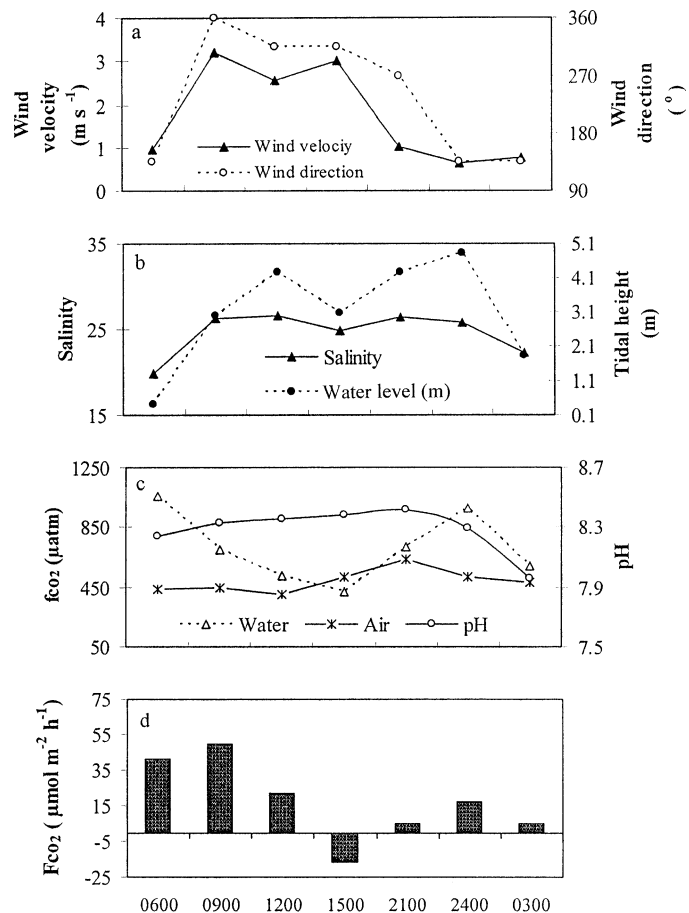


Fig. 2. Diurnal variation on 1–2 March 2001 at Sta. 2 (Saptamukhi R.). (a) Wind velocity and wind direction, (b) salinity and tidal height, (c) pH and f_{CO_2} in surface water and atmospheric f_{CO_2} , (d) carbon dioxide flux (F_{CO_2}).

sities (F_{CO_2} in $\mu\text{mol m}^{-2} \text{h}^{-1}$) across the water–atmosphere interface were calculated according to the expression $F = k \times L \times \Delta f$, where k is the exchange coefficient, L is the CO₂ solubility in $\text{mol m}^{-3} \text{atm}^{-1}$ and Δf is the fugacity difference between water and air, $[f_{\text{CO}_2(\text{water})} - f_{\text{CO}_2(\text{air})}]$. A positive F_{CO_2} value denotes flux from the water to the atmosphere and vice versa. Carbon dioxide exchange coefficients (k in cm h^{-1}) were estimated with the equation of Liss and Merlivat (1986), $k = 0.17u_{10} (660/S_c)^{2/3}$ for $u_{10} \leq 3.6$ and $k = (2.85u_{10} - 9.65)(660/S_c)^{0.5}$ for $3.6 < u_{10} \leq 13$, where u_{10} is the wind speed in m s^{-1} , S_c is the Schmidt number at the actual water temperature and salinity. The significance of the response of CO₂ flux was tested by multiple regression analysis with a stepwise variable selection. Independent variables were entered in order to account for seasonal variations of CO₂ flux.

Results and discussion

Diurnal variability—A set of examples of diurnal variations of wind velocity with direction, salinity with tidal height, f_{CO_2} and F_{CO_2} , is depicted in Fig. 2a–d, studied 1–2 March 2001 at Saptamukhi R. near Lothian island (Stn. 2). The temperature of surface water varied between 26°C and

Table 1. Seasonal variations of physicochemical and chemical properties of surface water (mean values of three stations with standard deviation).

Parameters	Monsoon	Postmonsoon	Premonsoon
Temperature (°C)	30.7 ± 1.2	26.9 ± 3.6	28.50 ± 3.56
Transparency (cm)	21 ± 6	64 ± 19	37 ± 26
Salinity	15.94 ± 3.89	14.90 ± 4.69	22.74 ± 4.28
Dissolved oxygen (mg L ⁻¹)	6.04 ± 0.94	6.38 ± 0.88	6.14 ± 0.38
(saturation %)	(88 ± 13)	(88 ± 11)	(89 ± 5)
DIN (μmol L ⁻¹)	18.40 ± 4.38	11.70 ± 7.65	12.10 ± 6.76
DIP (μmol L ⁻¹)	1.49 ± 0.67	1.01 ± 0.52	1.21 ± 0.48
Silicate (μmol L ⁻¹)	68.5 ± 13.5	75.9 ± 36.9	51.2 ± 32.2
pH	8.06 ± 0.16	8.28 ± 0.28	8.22 ± 0.16
TA (mequiv. L ⁻¹)	1.99 ± 0.32	1.80 ± 0.21	2.70 ± 0.35
R (mol C m ⁻² d ⁻¹)	0.20 ± 0.18	0.24 ± 0.18	0.19 ± 0.18
P (mmol C m ⁻² d ⁻¹)	6.95 ± 5.70	19.8 ± 10.4	12.2 ± 11.7
Phytoplankton (cells L ⁻¹)	4,045 ± 1,516	7,317 ± 4,854	5,145 ± 3,635

28°C and salinity (*S*) between 19.79 and 26.56. The depth of the water column at three sites varied between 9.7 and 15.2 m and there was almost no stratification in the water column. Tide was semidiurnal, with maximum amplitude of about 5.5 m. Secchi disc transparency varied between 7 and 99 cm, and low transparency was due to the turbidity of the water. Increased transparency of the water column was recorded during postmonsoon, with an average value of 64 ± 9.0 cm. Mean photic zone light energy was found to be 23.48 ± 4.5 klux, which was very close to the saturation light intensity of diatoms (10–20 klux). Average discharges of water from Farakka barrage during monsoon and postmonsoon were 2,975 and 1,875 m³ s⁻¹, respectively. Release of water during early premonsoon (February) was considerably decreased, to 1,100 m³ s⁻¹. Diurnal variations of air-flow showed land and sea breeze phenomenon, with a minimum value of land breeze from northwest to southeast (0.63 m s⁻¹) in nighttime and a maximum value of sea breeze from south/southeast to north/northwest direction (3.21 m s⁻¹) in daytime (Fig. 2a). $f_{\text{CO}_2(\text{air})}$ varied with time of day between 403 and 635 μatm. The minimum was found at 1200 h and the maximum at 2100 h, with a daily range of 232 μatm. Diurnal variation of $f_{\text{CO}_2(\text{air})}$ was strongly influenced by mangrove plant cover and was reduced when the air was directly from over the sea. Higher wind velocity and turbulence during the day caused mixing within the boundary layer and was responsible for the minimum value. Mukhopadhyay et al. (2002b) observed a positive correlation of $f_{\text{CO}_2(\text{air})}$ with Richardson number (*R*) and its values were found to be increasing in the atmosphere when there was an inversion condition in the Sundarban mangrove forest.

Considerable diurnal variation of $f_{\text{CO}_2(\text{water})}$ was found to occur with tidal variation of salinity and its maximum value of 1,062 μatm was observed in the early morning (0600 h) during the initial phase of low to high tide and its minimum value of 416 μatm in the afternoon (1500 h) during the last phase of high to low tide (Fig. 2b,c). The estimation of the CO₂ exchange coefficient is crucial for the estimation of carbon dioxide fluxes and is a matter open to debate (Raymond and Cole 2001). Its value of 4.57 ± 2.03 cm h⁻¹ was found at the wind velocity of 4.4 ± 0.79 m s⁻¹ and temperature of 29.39 ± 3.48°C in the study area. Clark et al. (1994) deter-

mined the gas exchange rate in the Hudson River using a dual tracer technique and proposed its values of ranging from 1 to 9 cm h⁻¹. Frankignoulle et al. (1996) used an exchange coefficient of 8.4 cm h⁻¹ at the experimental condition (*t* ~ 9°C) in the polluted estuary, the Scheldt. Cai and Wang (1998) suggested correlation of carbon dioxide to wind speed and physical mixing condition, and the reasonable value of exchange coefficient was considered 8 cm h⁻¹ for the purpose of tracing biogeochemical processes and constructing CO₂ budget in the estuarine waters of Satilla and Altamaha Rivers, Georgia. Wanninkhof and Knox (1996) observed that chemical enhancement had a minor effect on air–sea gas exchange coefficient of CO₂ under average oceanic turbulence conditions. The flux rates reported here are to be considered as estimates rather than absolute rates. The relative uncertainty on CO₂ flux measurements was found to be ±0.096. Variations of carbon dioxide fluxes from –16.2 to 49.9 μmol m⁻² h⁻¹ showed a distinct diurnal cycle (Fig. 2d). During daylight hours, photosynthesis led to a reduction in the $f_{\text{CO}_2(\text{water})}$ to a late afternoon (1500 h) minimum, and this was accompanied by a rise in pH of 8.38. During the dark hours, respiratory processes predominated and the $f_{\text{CO}_2(\text{water})}$ was increased while the pH fell to 7.96 (0300 h). In spite of higher $f_{\text{CO}_2(\text{water})}$, lower rates of CO₂ flux were observed during dark hours compared with that in the morning. This could be due to its lower evasion rate to the atmosphere during land breeze conditions. The diurnal estimate for the F_{CO_2} was found to be 13.78 μmol m⁻² h⁻¹.

Seasonal variability—Seasonal variations of physicochemical properties of surface waters are given in Table 1. Maximum and minimum air temperatures were recorded in May and January, being 35°C and 18.8°C, respectively. Salinity of this coastal water showed considerable dilution and decreased from 28.3 in May to 8.2 in October at Sta. 2. The surface water remained undersaturated with respect to dissolved oxygen throughout the year; saturation averaged 87.8%. DIN, calculated as (NO₃⁻ + NO₂⁻ + NH₄⁺), and DIP were considerably increased in monsoon. The average ratio of DIN/DIP was observed to be 11 ± 4, which was lower than the ratio of utilization by phytoplankton (Redfield ratio, 16:1). The ratios of availability to utilization were found to

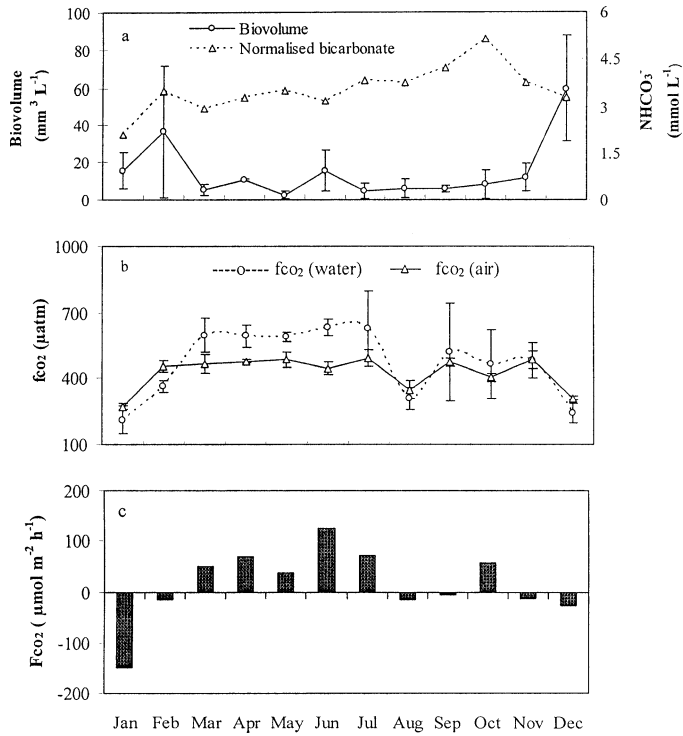


Fig. 3. Monthly variation of (a) phytoplankton biovolume and normalized bicarbonate, (b) f_{CO_2} in surface water and atmosphere, (c) monthly variation of average value of CO₂ flux for three stations.

be 0.69 to 1 for DIN and DIP, respectively. This indicates that nitrogen could be limiting before P. This ecosystem was also found heterotrophic in nature and community R was always found to be greater than gross primary P (Table 1). Total phytoplankton population ranged from 1,885 to 19,700 cells L⁻¹, with an average maximum of $7,317 \pm 4,854$ cells L⁻¹ in postmonsoon and an average minimum of $4,045 \pm 1,516$ cells L⁻¹ in monsoon. Correspondingly, phytoplankton biovolume varied with the seasons (Fig. 3a) between 0.49 and 86.52 mm³ L⁻¹. Biovolume decreased from a mean of 37.2 mm³ L⁻¹ in postmonsoon to 6.25 mm³ L⁻¹ in premon-

soon. Total number of phytoplankton genera were found to be 40 and noncalcifying algal species belonging to the genera *Coscinodiscus*, *Biddulphia*, *Ditylum*, *Thalassiosira*, *Lauderia*, *Nitzcha*, *Asterioella*, *Chaetoceros*, *Thalassionema*, *Thalassiothrix*, *Rizosolenia*, *Flagillaria*, *Planktonella*, *Skeletonema*, *Trichodesmium*, *Corethron*, *Hemiannulus*, *Navicula*, *Cyclotella*, *Guinerdia*, *Melosira*, *Gyrosigma*, *Roperia*, *Cerataulina*, *Ceratium*, *Protoperidium*, *Dinophysis*, *Surirela*, *Amphora*, *Bacillaria*, *Triceratium*, *Odentella*, and *Halosphaera*, were found to occur. Out of the 36 genera of diatoms, 1 genus of blue green algae, and 3 genera of dinoflagellates occurring throughout the year, only 10 species reached blooming proportion during postmonsoon between December and February. The average value of H' was found to be 0.87 ± 0.25 , indicating phytoplankton under high frequency of disturbance. Floder and Sommer (1999) reported the reduction of the value of H' to <2 when phytoplankton was imposed by high frequency of disturbance through increased supply of nutrients from deep water by mixing in the water column. Total surface area of phytoplankton species equal to $10^7 \mu\text{m}^2 \text{L}^{-1}$ was considered as bloom forming at any particular month (De et al. 1991), and monthly variations of bloom-forming species with their average cell surface area are given in Table 2.

Relative uptake of CO₂ and HCO₃⁻ in different species of marine diatoms acclimated to $f_{\text{CO}_2(\text{air})} \geq 360 \mu\text{atm}$ is of interest. Burkhardt et al. (2001) observed that *Thalassiosira weissflogii* and *Phaeodactylum tricorutum* acclimated to air-equilibrated CO₂ levels of $>360 \mu\text{atm}$ favored CO₂ uptake ($K_{1/2} \leq 5 \mu\text{mol CO}_2$) in comparison with HCO₃⁻ uptake ($K_{1/2} < 700 \mu\text{mol}$) during their maximum growth in a nutrient-enriched medium (f/2) of salinity 32. The present study revealed that nine other diatom species apart from *Thalassiosira subtilis* reached the blooming proportion during postmonsoon (Table 2) at $f_{\text{CO}_2(\text{air})/(\text{water})} \leq 360 \mu\text{atm}$ and salinity 14.9 ± 4.69 in mangrove water, and there was input flux of CO₂ from the atmosphere to mangrove water. But at high $f_{\text{CO}_2(\text{air})/(\text{water})} > 360 \mu\text{atm}$ during premonsoon ($S = 22.74 \pm 4.28$) and monsoon ($S = 15.94 \pm 3.89$), no species could reach the blooming proportion and there was an output flux

Table 2. Bloom-forming species, average cell surface area, blooming month, and minimum number required for bloom forming.

Sta. No.	Name	Bloom-forming month	Blooming concentration ($\times 10^7 \mu\text{m}^2 \text{L}^{-1}$)	Cell surface area [μm^2]	Minimum of cells to attain the blooming proportion ($10^7 \mu\text{m}^2 \text{L}^{-1}$) (Mani et al. 1986)
1	<i>Coscinodiscus gigas</i>	Dec	1.18	34,923	287
2	<i>Coscinodiscus radiatus</i>	Dec, Jan, Feb	1.06	11,187	894
3	<i>Coscinodiscus concinnus</i>	Dec, Feb	1.08	34,035	294
4	<i>Coscinodiscus eccentricus</i>	Jan, Feb	2.20	7,600	1,316
5	<i>Thalassiosira subtilis</i>	Dec, Jan	1.01	13,906	719
6	<i>Ditylum brightwelli</i>	Dec	1.40	11,970	835
7	<i>Rhizosolenia alata</i>	Feb	1.03	6,998	1,429
8	<i>Pleurosigma elongatum</i>	Dec	1.09	5,904	1,694
9	<i>Lauderia annulata</i>	Dec	1.06	3,465	2,887
10	<i>Chaetoceros affinis</i>	Feb	1.10	3,499	2,858

of CO₂ from mangrove water to the atmosphere. Monthly variations of NHCO₃⁻ (Fig. 3a) showed a progressive increase of its concentration during monsoon, with a maximum value of 5.1 mmol L⁻¹ in October; thereafter, its concentration decreased steadily during blooming of phytoplankton to an observed minimum of 2.08 mmol L⁻¹ in February. Therefore, blooming of these diatom species could decrease f_{CO_2} in water by HCO₃⁻ uptake. Crawford and Purdie (1997) suggested that the blooming of coccolithophorid, *Emiliania huxleyi*, would not cause an increase of $f_{\text{CO}_2(\text{water})}$ by utilizing HCO₃⁻ unless the ratio of calcification (C_{net}) to organic carbon production (P_{net}) exceeded the critical value of 1.5. Riebesell et al. (2000) observed the reduced $C_{\text{net}}:P_{\text{net}}$ ratio < 1.5 in two coccolithophorids, *E. huxleyi* and *Gephyrocapsa oceanica*, in response to increased atmospheric $f_{\text{CO}_2(\text{air})} > 360 \mu\text{atm}$. In contrast with coccolithophorids, diatoms showed reduced production at $f_{\text{CO}_2(\text{air})} > 360 \mu\text{atm}$ in spite of the occurrence of an increased concentration of nutrients in water during premonsoon and monsoon. This could be due to the poor transparency in the water column during premonsoon and monsoon as well as predation of phytoplankton by zooplankton, which showed maximum production during premonsoon (Sarkar et al. 1986).

Monthly variations of $f_{\text{CO}_2(\text{air})}$ and $f_{\text{CO}_2(\text{water})}$ are depicted in Fig. 3b. The $f_{\text{CO}_2(\text{water})}$ varied between 160 and 797 μatm and $f_{\text{CO}_2(\text{air})}$ between 255 and 520 μatm . Saturation values (expressed in %, i.e., 100% = equilibrium) were calculated as the ratios between water and atmosphere fugacity: $100 \times f_{\text{CO}_2(\text{water})}/f_{\text{CO}_2(\text{air})}$. Saturation of CO₂ with respect to atmosphere showed a significant decrease from 114% to 156% in premonsoon to 96.7% in monsoon and further decreased again to a minimum of 59% in postmonsoon. Average values of F_{CO_2} for three stations in every month are presented in Fig. 3c. Exchange flux of CO₂ was found reversed in postmonsoon, when phytoplankton reached blooming proportion and water showed increased values of pH and transparency along with decreased values of nutrients.

The significance of the response of CO₂ flux was tested by multiple regression analysis (Table 3). The dependent variable was F_{CO_2} and the independent variables were temperature (t), S , DIN/DIP ratio, ($P - R$), $f_{\text{CO}_2(\text{water})}$, and V . Statistical analysis revealed significant correlation between F_{CO_2} with independent variables tested ($R = 0.8$, $p = 0.002$). Linear terms t , DIN/DIP, ($P - R$) and $\ln f_{\text{CO}_2(\text{water})}$ were positive and influenced positive flux of CO₂ from water to atmosphere. Effects of linear terms S and V on F_{CO_2} were negative. As there was a little difference of salinity between monsoon and postmonsoon (Table 1), reversal of CO₂ flux from air to water was due to mainly a considerable increase of phytoplankton biovolume during postmonsoon.

Integrating over the year, the surface waters of the Sundarban mangrove (1,781 km²) exported 6.03×10^6 kg C, out of which 3.57×10^6 kg C was pumped out by the biological activity in the water annually. This corresponds to a CO₂ flux of $314.6 \mu\text{mol m}^{-2} \text{d}^{-1}$ ($13.8 \text{ kg C ha}^{-1} \text{ yr}^{-1}$) over the water area of the Sundarban. Had there been no change in the nature of this aquatic ecosystem from source to sink during eutrophication, the rate of emission of CO₂ from the water area would have been $33.85 \text{ kg C ha}^{-1} \text{ yr}^{-1}$. Richey et al. (2002) observed the CO₂ emission rate of 8.3

Table 3. Multiple regression* analysis with a stepwise variable selection. Dependent variable: F_{CO_2} , carbon dioxide flux ($\mu\text{mol m}^{-2} \text{ h}^{-1}$). Independent variables; t , temperature ($^{\circ}\text{C}$); S , salinity; DIN/DIP, ratio of dissolved inorganic nitrogen (DIN) with dissolved inorganic phosphate (DIP); ($P - R$), difference between net primary production and community respiration ($\text{mmol C m}^{-3} \text{ h}^{-1}$); $f_{\text{CO}_2(\text{water})}$, fugacity of CO₂ in water (μatm); V , phytoplankton cell volume ($\text{mm}^3 \text{ L}^{-1}$).

Predictor	R^2 (stepwise)	p	F	n
t	20.1	0.111	7.29	36
S	20.6	0.04	3.62	36
DIN/DIP	21.2	0.087	2.42	36
($P - R$)	23.3	0.129	1.97	36
$\ln f_{\text{CO}_2(\text{water})}$	59.2	<0.001	7.26	36
$\ln V$	59.2	0.001	5.81	36
$\ln f_{\text{CO}_2(\text{water})} \times S$	59.3	0.002	4.80	36
$\ln f_{\text{CO}_2(\text{water})} \times t$	63.0	0.002	4.68	36

* $F_{\text{CO}_2} = -1,561 + 11.6t - 3.76S + 5.28\text{DIN/DIP} + 3.7(P - R) + 300 \ln f_{\text{CO}_2(\text{water})} - 3.3 \ln V - 1.02 \times 10^{-4} \ln f_{\text{CO}_2(\text{water})} \times S - 3.18 \ln f_{\text{CO}_2(\text{water})} \times t$; $R^2 = 63\%$, $n = 36$, $F = 4.68$, $p = 0.002$, degrees of freedom = 8 and 22.

$\times 10^3 \text{ kg C ha}^{-1} \text{ yr}^{-1}$ from the fluvial environments of a 1.77 million km² quadrant of the low-gradient central Amazon basin, which yielded a flux of $0.9 \times 10^{12} \text{ kg C yr}^{-1}$ from the global area covered by humid tropical forests. European estuaries (Frankignoulle et al. 1996, 1998) also showed a high degree of supersaturation of $f_{\text{CO}_2(\text{water})}$, with an average value of $2,342 \pm 2,564 \mu\text{atm}$ and were sources of CO₂, with an average emission rate of $260 \pm 180 \text{ mmol m}^{-2} \text{ d}^{-1}$. Seasonally averaged partial pressure of surface water CO₂ in the subtropical gyres of the north ($15\text{--}20^{\circ}\text{N}$, 158°W) and south ($14\text{--}17^{\circ}\text{S}$, 150°W) Pacific Ocean were found to be significantly greater (331 ± 8.46 ; $324.5 \pm 7.62 \mu\text{atm}$) than that of atmosphere (326.5 ± 2.9 ; $322.6 \pm 0.95 \mu\text{atm}$) and a net flux of CO₂ from the sea to the atmosphere of the order of $0.274 \text{ mmol m}^{-2} \text{ d}^{-1}$ was reported by Weiss et al. (1982). Estimates that the tropical mangrove waters is a net carbon source is consistent with recent calculations from global inverse modeling, which implies that the tropics are at least in balance with the atmosphere if not net source (Gurney et al. 2002). Extrapolating over the global area ($13.9 \times 10^4 \text{ km}^2$) covered by mangrove forests (Mastaller 1996) with our estimate of aerial evasion rates for the Sundarban yields a flux of roughly $0.19 \times 10^9 \text{ kg C yr}^{-1}$, which is about 0.019% of global evasion over humid tropical forests.

References

- AYUKAI, T., D. MILLER, E. WOLANKSI, AND S. SPAGNOL. 1998. Fluxes of nutrients and dissolved and particulate organic matter in 2 mangrove creeks in north-eastern Australia. *Mangr. Salt Marsh* **2**: 223–230.
- BRADSHAW, A. L., AND P. G. BREWER. 1988. High precision measurements of alkalinity and total carbon in seawater by potentiometric titration: 2. Measurements of standard solution. *Mar. Chem.* **34**: 155–162.
- BURKHARDT, S., G. AMOROSO, U. RIEBESELL, AND D. SULTEMEYER. 2001. CO₂ and HCO₃⁻ uptake in marine diatoms acclimated to different CO₂ concentrations. *Limnol. Oceanogr.* **46**: 1378–1391.

- CAI, W., AND Y. WANG. 1998. The chemistry, fluxes, and sources of carbon dioxide in the estuarine waters of the Satilla and Altamaha Rivers, Georgia. *Limnol. Oceanogr.* **43**: 657–668.
- CLARK, J. F., R. WANNINKHOF, P. SCHLOSSER, AND H. J. SIMPSON. 1994. Gas exchange rates in the tidal Hudson River using a dual tracers technique. *Tellus* **46B**: 274–285.
- CLOUGH, B. 1998. Mangrove forest productivity and biomass accumulation in Hinchinbrook Channel, Australia. *Mangr. Salt Marsh* **2**: 191–198.
- CRAWFORD, D. W., AND D. A. PURDIE. 1997. Increase of PCO₂ during bloom of *Emiliania huxleyi*: Theoretical consideration on the asymmetry between acquisition of HCO₃⁻ and respiration of free CO₂. *Limnol. Oceanogr.* **42**: 365–372.
- DE, T. K., S. K. GHOSH, T. K. JANA, AND A. CHOUDHURY. 1991. Phytoplankton bloom in the Hooghly estuary. *Ind. J. Mar. Sci.* **20**: 134–137.
- DITTMAR, T., AND R. J. LARA. 2001. Do mangroves rather than rivers provide nutrients to coastal environments, South of the Amazon River? Evidence from long term flux measurements. *Mar. Ecol. Prog. Ser.* **213**: 67–77.
- FLODER, S., AND U. SOMMER. 1999. Diversities in planktonic communities: An experimental test of the intermediate disturbance hypothesis. *Limnol. Oceanogr.* **44**: 1114–1119.
- FRANKIGNOULLE, M., AND OTHERS. 1998. Carbon dioxide emission from European estuaries. *Science* **282**: 434–436.
- , I. BOURGE, AND R. WOLLAST. 1996. Atmospheric CO₂ fluxes in a highly polluted estuary (the Scheldt). *Limnol. Oceanogr.* **41**: 365–369.
- GHOSH, S. K., T. K. JANA, B. N. SINGH, AND A. CHOUDHURY. 1987. Comparative study on carbon dioxide system in virgin and reclaimed mangrove waters of Sundarban during freshet, Mahasagar. *Bull. Natl. Inst. Oceanogr.* **20**: 155–161.
- , B. N. SINGH, C. CHAKRABORTY, A. SAHA, R. L. DAS, AND A. CHOUDHURY. 1990. Mangrove litters production in tidal creek of Lothian Island of Sundarbans, India. *Ind. J. Mar. Sci.* **19**: 292–293.
- GRASSHOFF, K. 1983. Determination of salinity and oxygen, p. 31–72, and Determination of nutrients, p. 125–187. *In* K. Grasshoff, M. Ehrhard, K. Kremling [eds.], *Methods of seawater analysis*. Verlag Chemie.
- GOYET, C., AND A. POISSON. 1989. New determination of acid dissociation constants in seawater as a function of temperature and salinity. *Deep Sea Res.* **36**: 1635–1654.
- GURNEY, R. R., AND OTHERS. 2002. Towards robust regional estimates of CO₂ sources and sinks using atmospheric transport models. *Nature* **415**: 626–630.
- HASLE, G. R., AND E. E. SYVERTSEN. 1997. Marine diatoms, p. 5–385. *In* C. R. Tomas [ed.], *Identifying marine phytoplankton*. Academic.
- HOPE, D., S. M. M. PALMER, F. PRILLET, AND J. J. DAWRON. 2001. Carbon dioxide and methane emission from a temperate peat land stream. *Limnol. Oceanogr.* **46**: 847–857.
- IGBP. 1995. Land–ocean interaction in the coastal zone, J. C. Perret and J. D. Milliman [eds.]. IGBP report 33, Stockholm, p. 16.
- KELLAR, P. E., S. A. PAULSON, AND L. J. PAULSON. 1980. Methods for biological, chemical and physical analysis in reservoirs. *Tech. Rep. 5*, Lake Mead Limnological Res. Centre, Univ. Nevada.
- KEMPE, S., AND PELGER. 1991. Sinks and sources of CO₂ in coastal seas: The North Sea. *Tellus* **43B**: 224–235.
- LISS, P. S., AND L. MERLIVAT. 1986. Air sea gas exchange rates: Introduction and synthesis, p. 113–129. *In* P. Buat-Menard [ed.], *The role of air sea exchange in geochemical cycling*. D. Reidel.
- MANI, P. K., K. KRISHNAMURTHY, AND R. PALANIAPPAN. 1986. Ecology of phytoplankton blooms in the Vellar Estuary, East Coast of India. *Ind. J. Mar. Sci.* **15**: 24–28.
- MASTALLER, M. 1996. Destruction of mangrove wetlands—causes and consequences. *Nat. Res. Dev.* **43/44**: 37–57.
- MILLERO, F. J. 2000. The carbonate system in marine environments, p. 41. *In* A. Gianguzza, E. pelizzetti, and S. Sammartano [eds.], *Chemical process in marine environments*. Springer-Verlag.
- MISRA, S., A. K. DUTTA, A. GHOSH, AND A. CHOUDHURY. 1985. Oxidation of oleanolic acid of *Avicennia officinalis* leaves to oleanonic acid in the natural environment of Sunarbans mangrove ecosystem. *J. Chem. Ecol.* **11**: 339–343.
- MUKHOPADHYAY, S. K., H. BISWAS, T. K. DE, S. SEN, AND T. K. JANA. 2002a. Seasonal effects on air water of carbon dioxide exchange in the Hooghly estuary, NE coast of Bay of Bengal, India. *J. Environ. Monit.* **4**: 549–552.
- , H. BISWAS, T. K. DE, S. SEN, B. K. SEN, AND T. K. JANA. 2002b. Impact of Sundarban mangrove biosphere on the carbon dioxide and methane mixing ratio at the NE coast of Bay of Bengal, India. *Atmos. Environ.* **36**: 629–638.
- QUAY, P. D., B. TILBROOK, AND C. S. WONG. 1992. Oceanic uptake of fossil fuel CO₂: Carbon-13 evidence. *Science* **256**: 74–79.
- RAYMOND, P. A., AND J. J. COLE. 2001. Gas exchange in rivers and estuaries: Choosing a gas transfer velocity. *Estuaries* **24**: 312–317.
- RICHEY, J. E., J. M. MALACK, A. K. AUFDAN KAMPE, V. M. BALLESTER, AND L. L. HESS. 2002. Out gassing from Amazonian rivers and wetlands as a large tropical source of atmospheric CO₂. *Nature* **416**: 617–620.
- RIEBESELL, U., I. ZONDERVAN, B. ROST, P. D. TORTELL, R. E. ZEEBE, AND F. M. M. MOREL. 2000. Reduced calcification in marine plankton in response to increased atmospheric CO₂. *Nature* **407**: 364–367.
- ROY, S., R. E. ULANOWICZ, N. C. MAJEE, AND A. B. ROY. 2000. Network analysis of a benthic food web model of a partly reclaimed island in the Sundarban mangrove ecosystem, India. *J. Biol. Sys.* **8**: 263–278.
- SARKAR, S. K., B. N. SING, AND A. CHOUDHURY. 1986. Seasonal distribution of copepods in the Hooghly Estuary, West Bengal. *Ind. J. Mar. Sci.* **15**: 177–180.
- SCHIMEL, D., I. G. ENTING, M. HEIMANN, T. M. L. WIGLEY, D. RAYNAUD, D. ALVES, AND U. SIEGENTHALER. 1995. Radiation forcing of climate change and an evaluation of the IPCC IS 92 emission scenarios, p. 35–71. *In* J. T. Houghton, L. G. Meira Filho, J. Bruce, Lee Hoesung, B. A. Callander, E. Haites, N. Harris, and K. Markell [eds.], *Climate change 1994*, v. 339. Cambridge Univ. Press.
- SHANNON, C. E., AND W. WEAVER. 1963. *The mathematical theory of communication*. Univ. Illinois Press.
- STRICKLAND, J. D. H., AND T. R. PARSONS. 1972. *A practical handbook of seawater analysis*, 2nd ed. Bull. Fish. Res. Board Canada.
- TANS, P. P., I. Y. FUNG, AND T. TAKAHASHI. 1990. Observational constraints on the global atmospheric CO₂ budget. *Science* **247**: 1431–1438.
- WANNINKHOF, R., AND M. KNOX. 1996. Chemical enhancement of CO₂ exchange in natural waters. *Limnol. Oceanogr.* **41**: 689–697.
- WEISS, R. F. 1974. Carbon dioxide in water and seawater; the solubility of a non ideal gas. *Mar. Chem.* **2**: 203–215.
- , R. A. JAHNKE, AND C. D. KEELING. 1982. Seasonal effects of temperature and salinity on the partial pressure of carbon dioxide in seawater. *Nature* **300**: 511–513.

Received: 7 December 2002
 Accepted: 25 July 2003
 Amended: 8 September 2003